

Using high-resolution lidar point clouds to evaluate 1-3 arc second global digital elevation models

Peter L. Guth[§]

Department of Oceanography
 United States Naval Academy
 572C Holloway Road
 Annapolis MD 21402 USA

[§] pguth@usna.edu

Abstract—Widely available lidar point clouds have 2-10 returns per m², which translates to 1500-10,000 points corresponding to each elevation posting in a 1” (arc second) digital elevation model (DEM). The lidar point cloud approximates the 3D earth surface observed by the visible, near infrared, and radar sensors used to create the DEMs, and allows estimation of the canopy penetration by the sensor. Canopy is broadly defined as the range of elevations within the 1” cell including effects from vegetation, slope, and man-made features. In open terrain, the SRTM, ALOS, and ASTER global DEMs approximate the ground surface. With significant canopy, the DEMs are closer to the top of the canopy, with the SRTM the lowest near the midpoint of the canopy. The ASTER does the poorest job of matching the lidar surface.

freely available lidar data. For free near global coverage, the best resolution is 1” (arc second, approximately 30 m). Table 1 shows 4 DEMs at this scale, and three additional DEMs at 3” (about 90 m). All use the WGS84 datum, and all have orthometric heights except for TandemX which has ellipsoidal heights.

I. INTRODUCTION

The digital elevation model (DEM) serves as the backbone for many studies in earth science, hydrology, land use planning and management, and military operations. The goal of most DEMs is to sample the bare earth, or digital terrain model (DTM), the land’s surface stripped of vegetation and man-made features like buildings and power lines. Lidar provides extremely high resolution on the order of 1 m grid spacing and can produce either a DTM or a DSM, but only a few countries currently have

The SRTM, ASTER, and ALOS DEMs have comparable scales, and rely on three independent creation methods. SRTM was created during a single 11 day radar mission, while ASTER and ALOS used multiple collections of stereo imagery over multiple years and all seasons. At their scale, temporal and seasonal changes should not greatly affect most of their coverage area. GSDEM and MERIT attempt to deal with shortcomings in the data, notably holes, and create an improved, merged data set, while Tandem X and Copernicus DEM provide lower resolution free data based on much higher resolution commercial data.

This paper will show how well the SRTM, ASTER, and ALOS DEMs manage to penetrate canopy by comparing their elevations with high density lidar point clouds which record data from the top of the canopy to the ground, and if the DEMs are DTMs or DSMs.

Table 1. Free global DEMs with 1-3” spacing

DEM	Spacing	Source	Producer	Precision	Years Acquired	Ref	Download
SRTM (v3)	1”	Radar	NASA	Integer	2000 (11 days)	[1]	[2]
ASTER GDEM	1”	Stereo NIR imagery	NASA / JAXA	Integer	2000-2013	[3]	[4]
ALOS World 3D AW3D30	1”	Stereo pan imagery	JAXA	Integer	2006-2011	[5]	[6]
GSDEM-30	1”	Radar + stereo NIR imagery + stereo pan imagery	China	Float		[7]	[8]
MERIT	3”	Radar + Stereo pan imagery	Univ. Tokyo	Float		[9]	[10]
Tandem_X	3”	Radar	DLR	Float	2010-2015	[11]	[12]
Copernicus DEM	3”	Edited radar (Tandem_X)	Airbus/ESA	Float		[13]	

Peter Guth (2020) Using high-resolution lidar point clouds to evaluate 1-3 arc second global digital elevation models:

in Massimiliano Alvioli, Ivan Marchesini, Laura Melelli & Peter Guth, eds., *Proceedings of the Geomorphometry 2020 Conference*, doi:10.30437/GEOMORPHOMETRY2020_31.

Table 2. Lidar data sets used for comparison with 1” global DEMs

AREA	LOCATION	1" CELLS	Points per cell	Lidar elevation range (m)	SRTM slope (%) and std dev	Canopy height (m) and std dev
ANNAP	N38.99° W76.49°	7911	9942	-38 to 79	3.05±3.04	15.97±11.53
BLED	N46.37° E14.10°	3808	8050	474 to 642	8.58±12.62	17.12±15.28
CA	N39.85° W123.77°	12,606	7178	161 to 671	34.07±13.51	43.62±8.95
CO	N39.32° W106.28°	12,090	1910	3107 to 3704	25.46±13.87	20.76±10.34
ICOD	N28.37° W16.70°	38,913	1577	-2 to 1005	15.65±12.66	15.97±11.45
OAHU	N21.50° W158.19°	15,477	2984	95 to 988	40.60±26.38	36.03±19.31
VA	N38.62° W78.36°	3087	5753	582 to 994	32.55±13.65	32.05±6.76
VEGAS	N36.51° W115.08°	3176	4969	1772 to 2159	31.96±13.83	16.54±6.15

Within a lidar point cloud, the range of elevations in any region depends on the slope of the terrain and height of features above the ground sampled by the lidar. Trees represent the predominant above ground features, but modern lidars also increasing have many returns from utility lines which are not identified by the national mapping agencies in the delivered lidar products. These features would also have been imaged by the radar, visible, and near IR sensors used for global DEM generation, and this research seeks to quantify the penetration achieved by the sensors and see how far they depart from the desired DTM and instead reflect a digital surface model (DSM).

II. METHODS

Lidar point clouds in LAS or LAZ format from national mapping agencies cover a range of environments (Table 2) [14,15,16,17]. One arc second Geotiff DEMs [2,4,6] cover the areas with the lidar data sets. Lidar points classified as low or high noise were excluded from analysis, but all other returns are included. With the region of lidar coverage, the lidar points corresponding to each 1”x1” grid cell in the DEM were extracted and statistics computed. These points represent the “canopy” of the cell and include the ground, buildings, vegetation, power lines, and any other features. The canopy also includes the range of elevations due to the slope of the ground, and provides an estimate of ground truth for what is present in the cell. The sensors creating the global DEMs imaged the surface represented by the cloud and derived a single elevation, at a different time, season, or even a composite of multiple views over a period of years.

Figure 1 shows a 1” single cell, and the uneven distribution of lidar returns within its canopy and elevations from the three global DEMs. Figure 2 depicts the canopy penetration along a profile showing the lidar classifications with ground, buildings,

and vegetation. Figure 3 shows a simplified, longer profile with the upper and lower limits of the lidar point cloud and the three global DEMs.

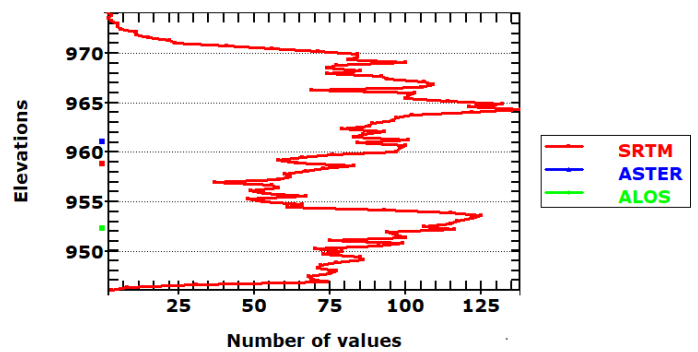


Figure 1. Point cloud density for 1”x1” cell, and elevation from 3 global DEMs on the left axis.

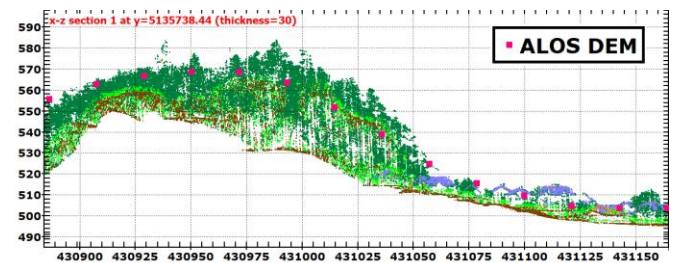


Figure 2. Slice through classified point cloud with the ALOS grid postings.

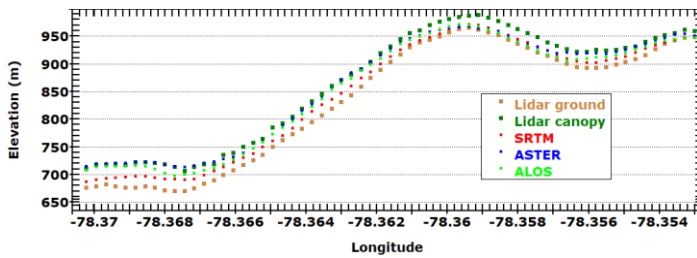


Figure 3. Profile of the ground and canopy top, and the DEM elevations.

Figures 1-3 reveal the micro-scale details of canopy penetration. To scale up the analysis, Figure 4 shows the proportion of the cells where the DEM elevation was above, within, or below the point cloud. This varies greatly by location and with the DEM. Figure 5 shows the distribution of the DEM elevations within the canopy of the lidar points. The elevations are scaled from 0 at the base of the canopy (lowest lidar elevation in the cell) to 1 at the canopy top (highest elevation in the cell); the green shading highlights this range. A value of 2 indicates the DEM point is twice the height of the canopy, and a value of -1 indicates the DEM elevation post was the height of the canopy below the ground level. As an alternative scaling, the percentile scaling within the point used the density of returns, from 0% at the ground to 100% at the top of the canopy. This is not linear, as

seen in Figure 1 when there are peaks in density at 954 and 964 m, and very few returns above 970 m. The percentile scaling shows the same general patterns at the linear scaling in Fig. 5, but cannot extrapolate scaling for point outside the canopy range.

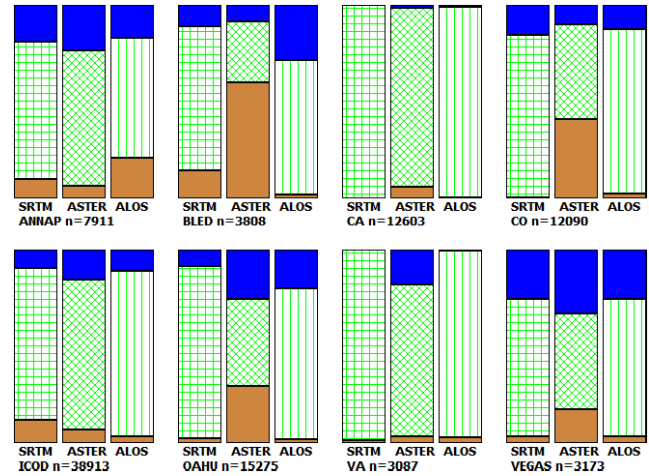


Figure 4. Proportion of DEM elevations above (blue), within (green), and below (brown) the point cloud.

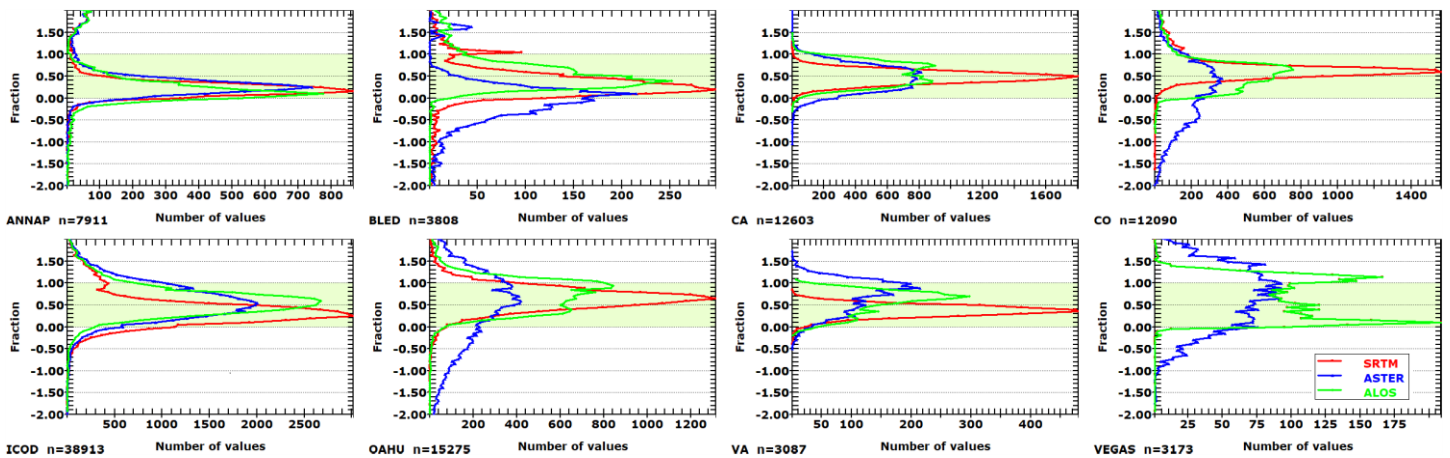


Figure 5. Distribution of the DEM postings within a linear scaling of the point cloud for the eight areas in Table 2. For the Vegas area SRTM is identical to ALOS.

III. RESULTS AND CONCLUSIONS

Canopy penetration with the sensors used for the SRTM, ALOS, and ASTER DEMs varies with the terrain. The elevations are closest to the ground, defined by the lowest lidar points, in relatively open terrain with many man-made features (ANNAP, BLED, and ICOD). These also contain the least steep terrain.

ASTER consistently shows the most points that do not lie within the lidar-defined canopy. It has many points (BLED, CO, OAHU, and VEGAS) below the ground level defined by the lidar data. A number of studies have found ASTER's quality problematic [19, 20], but it remains useful for its ability to image terrain where SRTM has challenges.

In forested terrain (CA, CO, OAHU, VA), SRTM elevations show a sharp peak concentration in about the middle of the canopy defined by the lidar. The ALOS and ASTER show a less clearly defined peak, with a tendency to record a higher position within the canopy implying that the radar achieved better penetration through vegetation. The northern hemisphere winter acquisition probably enhanced signal penetration for SRTM; ALOS and ASTER collected over a period of years and have variable season of acquisition. ALOS has a tendency for a bimodal distribution of returns from the canopy.

Future work will concentrate on the following extensions:

- Comparisons of grids created from lidar with global DEMs. The lidar can create either a DSM, DTM, or NVS (non-vegetated surface), and the global DEM would be closest to a DSM, so the comparison is not straight forward, and also requires a resampling method (min, max, mean, median, closest to the center of the cell). These regions had an average of 1500 to 10,000 points per 1" (about 900 m²) cell, allowing a lot of statistical manipulation of the data.
- Comparison of the global DEM with clouds composed only of the lidar points classified as ground. While the ground remains the goal for the global DEMs, their sensors do not readily penetrate vegetation or buildings.
- Incorporating land cover classification into the analysis.
- Adding the freely available 90 m global DEMs to the analysis.

IV. ACKNOWLEDGMENTS

All analysis was done with the MICRODEM program [21], including new code to automate the analysis steps. I thank Ian Evans for a very helpful review.

REFERENCES

- [1] Farr, T. G., et al., 2007. "The Shuttle Radar Topography Mission". *Rev. Geophys.*, 45, RG2004, doi:10.1029/2005RG000183.
- [2] USGS, 2020, "Earth explorer home". <https://earthexplorer.usgs.gov/>
- [3] NASA/METI/AIST/Japan Space systems, and U.S./Japan ASTER Science Team, 2001. "ASTER DEM Product [Data set]". NASA EOSDIS Land Processes DAAC. Accessed 2020-02-03 from <https://doi.org/10.5067/ASTER/AST14DEM.003>
- [4] Earthdata, 2020. "EARTHDATA Search". <https://search.earthdata.nasa.gov/search/>
- [5] Tadono, T., Takaku, J., Tsutsui, K., F. Oda, and Nagai, N., 2015. "Status of ALOS World 3D (AW3D) global DSM generation. Proceeding 2015 IEEE International Geoscience and Remote Sensing Symposium (IGARSS), 3822-3825, doi:10.1109/IGARSS.2015.7326657
- [6] JAXA, 2020. "Precise Global Digital 3D Map "ALOS World 3D" Homepage", https://www.eorc.jaxa.jp/ALOS/en/aw3d/index_e.htm
- [7] Yue, L., Shen, H., Liu, L., Yuan, Q., and Zhang, L., 2019. "A Global Seamless DEM Based on Multi-Source Data Fusion (GSDEM-30): Product Generation and Evaluation". <https://www.preprints.org/manuscript/201906.0036/v1>
- [8] http://sendimage.whu.edu.cn/res/DEM_share/ Link broken Feb.29, 2020.
- [9] Yamazaki, D., D. Ikeshima, R. Tawatari, T. Yamaguchi, F. O'Loughlin, J. C. Neal, C. C. Sampson, S. Kanae, and P. D. Bates, 2017. "A high-accuracy map of global terrain elevations". *Geophys. Res. Lett.*, 44, 5844-5853, doi:10.1002/2017GL072874.
- [10] Yamazaki, D., 2018, "MERIT DEM: Multi-Error-Removed Improved-Terrain DEM". http://hydro.iis.u-tokyo.ac.jp/~yamada/MERIT_DEM/index.html
- [11] Rizzoli, P., Martone, M., Gonzalez, C., Wecklich, C., Borla Tridon, D., Brautigam, B., Bachmann, M., Schulze, D., Fritz, T., Huber, M., Wessel, B., Krieger, G., Zink, M., and Moreira, A., 2017. "Generation and performance assessment of the global TanDEM-X digital elevation model". *ISPRS Journal of Photogrammetry and Remote Sensing*, Vol 132, pp. 119-139.
- [12] DLR, 2020. "The TanDEM-X 90m Digital Elevation Model". <https://geoservice.dlr.de/web/dataguide/tdm90/#access015>
- [13] Airbus, 2020. "Copernicus DEM product handbook". https://spacedata.copernicus.eu/documents/12833/20611/GEO1988-CopernicusDEM-SPE-002_ProductHandbook_11.00/150167c3-3687-4f8e-9745-658ec29b3df0
- [14] Agencia rs za Okolje, 2020. "LIDAR". http://gis.arso.gov.si/evode/profile.aspx?id=atlas_voda_Lidar@Arso
- [15] Centro del Descargas, 2020. "Products". http://centrodedescargas.cnig.es/CentroDescargas/locale?request_local_e=en
- [16] OpenTopography, 2020. <https://opentopography.org/>
- [17] USGS, 2020. "TNM download". <https://viewer.nationalmap.gov/basic/>
- [18] Maryland, 2020. "Maryland statewide lidar download tool". <https://lidar.geodata.md.gov:8443/ExpressZip>
- [19] Guth, P.L., 2010. "Geomorphometric comparison of ASTER DEM and SRTM". *Join Symposium of ISPRS Technical Commission IV*, Orlando, FL, p. 10.
- [20] Hengl, T., and Reuter, H.I., 2011, How accurate and usable is GDEM? A statistical assessment of GDEM using Lidar data: In *Geomorphometry 2011*, edited by T. Hengl, I. S. Evans, J. P. Wilson and M. Gould, 45-48. Redlands, CA, 2011. <http://www.geomorphometry.org/HenglReuter2011>
- [21] Guth, P.L., 2009, *Geomorphometry in MICRODEM*. In Hengl, T., Reuter, H.I. (eds), *Geomorphometry: concepts, software, applications. Developments in Soil Science Series*, Elsevier, p.351-366. Program at <https://www.usna.edu/Users/oceano/pguth/website/microdem/microdemdo wn.htm> .